Simulation of Si/SiGe Micro-Cooler by Thermal Quadrupoles Method

Y. Ezzahri [*(a)], S. Dilhaire [(a)], S. Grauby [(a)], L. D. Patiño-Lopez [(a)], W. Claeys [(a)],
Y. Zhang [(b)], Z. Bian [(b)], and A. Shakouri [(b)],
(a) Centre de Physique Moléculaire Optique et Hertzienne (CPMOH)
Université de Bordeaux, 351 cours de la libération, 33405 Talence
Cedex, France.
(b) Jack Baskin School of Engineering, University of California at Santa Cruz
Santa Cruz, CA 95064-1077, USA
*Corresponding author. Tel: +33-5-40-00-27-93. Fax: +33-5-40-00-69-70.
E-Mail address: y.ezzahri@cpmoh.u-bordeaux1.fr

Abstract

A new method based on thermal quadrupoles is presented to model the behavior of a single stage Si/SiGe micro-cooler in AC operating regime. The cold side temperature is calculated for different excitation frequencies, current magnitudes and device sizes. The sensitivity and precision of this method come from its analytical expressions, which are based on the solution of the Fourier heat equation in Laplace space. We assume that the thermal properties of the device are temperature independent. Action of each layer is represented by a matrix which relates the temperature-flux vectors at both sides in the frequency domain. A comparison of the model with experimental reflectometry techniques is also presented. Performance of Si/SiGe micro-coolers can be optimized by a combination of optical characterization techniques and the thermal quadrupoles simulation.

I. Introduction

Thermoelectric materials are frequently used in several fields of microelectronics and optoelectronics. In the last ten years, low dimensional cooling devices have attracted a lot attention due to an increasing demand for localized cooling and temperature stabilization in microelectronic and optoelectronic devices. The low dimensional materials have manifested very interesting thermoelectric properties, enabling them to have a figure of merit, ZT, exceeding 1 at room temperature. One of those materials is a SiGe/Si superlattice structure with a better ZT at room temperature though SiGe has been known for a good thermoelectric material for high temperature applications [1].

Si-based microcoolers are attractive for their potential monolithic integration with Si microelectronics. D. Vashaee et al [2, 3] had proposed a model to simulate the behavior of a Si/SiGe microcooler, but they were limited to the DC regime. In this paper, we extend the model to the AC regime using the Thermal Quadrupoles Method (TQM) [4]. This method has been used to model the behavior of a conventional thermoelectric module (Bi_2Te_3) [5], it consists of an analytical model which predicts electric and thermal responses at the first and second harmonic, thus making it possible to distinguish, in some cases, the Peltier effect from the Joule effect. The first appears at the same frequency as the operating current, whereas the second appears at the double frequency. The precision of this method allows its application in the detailed characterization of thermoelectric material properties.

II. Sample description

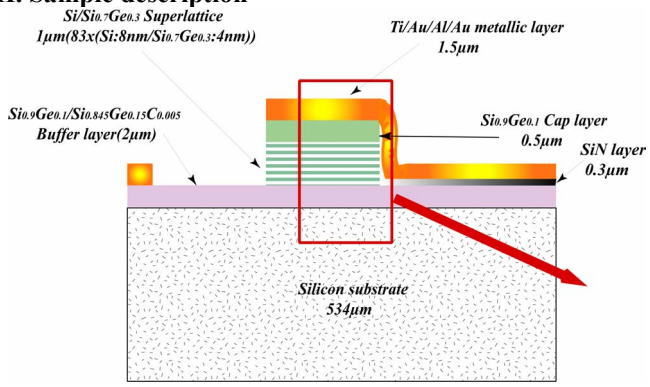

Figure 1: schematic diagram of the microcooler cross section.

Figure 1 shows a schematic cross-sectional view of the Si/SiGe superlattice microcooler we have experimentally studied. It is constituted of 1µm thick superlattice layer with the structure of 83×(8nm Si/4nm $Si_{0.7}Ge_{0.3}$) and doping concentration of 5×10^{19} cm^{-3}. The buffer layer is a 1µm thick $Si_{0.9}Ge_{0.1}$ film followed by 1µm thick $Si_{0.9}Ge_{0.1}/Si_{0.845}Ge_{0.15}C_{0.005}$ superlattice with the same doping concentration as the superlattice, the cap layer, in total, is 0.5µm, consisting of a 0.25µm $Si_{0.9}Ge_{0.1}$ film with a doping concentration of 5×10^{19} cm^{-3} followed by another 0.25µm film with a higher doping concentration of 2×10^{20} cm^{-3} [6]. The most important part of the device is the superlattice layer. In addition to thermionic emission, it can also reduce the thermal conductivity to prevent the heat flowing back to the cold junction from the substrate. The buffer layer on top of the Si substrate was included in order to reduce the lattice mismatch strain between the substrate and the superlattice [7]. The cap layer with the higher doping concentration of 2×10^{20} cm^{-3}, was included in order to improve the ohmic-contact between the metal and the semiconductor. The SiN insulating layer is added to prevent any current leaking from the probe into substrate, thus the current path is confined from probe to the top of the superlattice, before being distributed into the substrate. . The superlattice was grown in a molecular beam epitaxy (MBE) machine on a five inch diameter (001)-oriented Si substrate, and p-type doped to 0.003-0.007Ω.cm with boron. A 1.5µm Ti/Al/Ti/Au layer was evaporated on top of the sample for electrical contact.

III. Thermoelectric and Thermionic cooling

In Si/SiGe microcooler, Peltier cooling occurs at the metal-layer/Cap-layer junction and interface between the

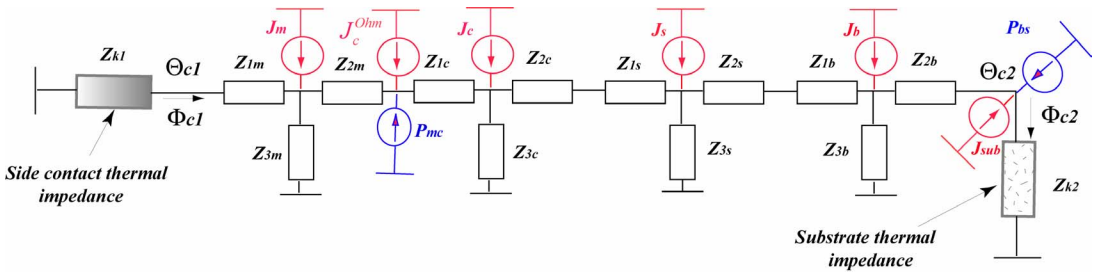

Figure 2: Thermal quadrupole system of the microcooler.

buffer-layer and substrate when the device is fed by a current. The density of heat that can be exchanged with the surrounding medium is characterized by the effective Seebeck coefficient at these junctions, moreover, it is proportional to both current intensity and junction temperature.

Assuming small current densities, we can define an effective Seebeck coefficient for thermionic cooling by analogy to thermoelectric cooling. The density of heat can be considered as linearly dependent on the current [8]. In our model, we assume that the Seebeck coefficient value takes into account both thermoelectric and thermionic phenomena.

IV. Thermal quadrupoles model

The thicknesses of the different layers, including the superlattice layer, are several order of magnitude larger than the mean free path of both electrons and phonons. We can hence assume a diffusive regime, and Fourier Diffusive Classical Heat Equation (FDCHE) is by consequence applied to describe heat transport inside the sample.

In adiabatic conditions, the resolution of the FDCHE in a passive, linear, and isotropic medium for a one-dimensional heat transfer with the Laplace transform gives a linear relation between temperature- flux vectors at both ends, this relation can be put in a matrix form:

$$\begin{pmatrix}\theta_{in}\\ \phi_{in}\end{pmatrix}=\begin{pmatrix}A & B\\ C & D\end{pmatrix}\begin{pmatrix}\theta_{out}\\ \phi_{out}\end{pmatrix}=\begin{pmatrix}ch(qe) & \frac{1}{K}sh(qe)\\ Ksh(qe) & ch(qe)\end{pmatrix}\begin{pmatrix}\theta_{out}\\ \phi_{out}\end{pmatrix}=\mathrm{M}\begin{pmatrix}\theta_{out}\\ \phi_{out}\end{pmatrix}$$

where $q=\sqrt{\frac{p}{\alpha}}$, p is Laplace parameter, $K=\beta Sq$, and $\alpha=\frac{\beta}{\rho C}$ is thermal diffusivity of the medium, β, ρC, e and S are respectively thermal conductivity, specific heat per unit volume, the thickness of the medium and its cross section area.

The characteristics of this matrix, namely A=D, and Det(M)=1, are typical for a transfer matrix of a symmetrical system. Such a system remains unchanged if one reverses the axis of propagation, and can be related to the properties of a passive four-terminal network, which can be represented by three impedances connected in the "T" circuit, as shown in figure 2.

We must note here that ground level corresponds to room temperature, the impedances are thermal, and they are a function of the transfer matrix coefficients:

$$Z_1=Z_2=\frac{A-1}{C},\ Z_3=\frac{1}{C}$$

This representation by impedances corresponds to the relation between boundary conditions.

The thickness of the whole structure is very small compared to that of the substrate; moreover, all Peltier sources are uniform on all junction plans, the heat transfer across the sample can be considered one-dimensional. Side and surface losses by convection-radiation will be neglected and adiabatic conditions are assumed. This can be justified due to the small dimensions of the microcooler and marginal cooling temperature reduction. Our structure is formed of four essential layers; the transfer matrix of each layer can be put in the form:

$$\begin{pmatrix}\theta_{in}\\ \phi_{in}\end{pmatrix}=\begin{pmatrix}A_i & B_i\\ C_i & D_i\end{pmatrix}\begin{pmatrix}\theta_{out}\\ \phi_{out}\end{pmatrix}-\begin{pmatrix}Z_{1i}J_i\\ J_i\end{pmatrix}$$

where $A_i=ch(qe_i)=D_i$, $B_i=\frac{1}{K_i}sh(qe_i)$, and $C=K_i sh(qe_i)$.

The term J_i indicates the internal conventional Joule source inside each layer, and is given by:

$$J_i=\frac{R_i I_e^2}{2e_i}\int_0^{e_i} ch(qz)dz=\frac{1}{2}R_i I_e^2\frac{sh(qe_i)}{qe_i} \qquad (1)$$

(1.1)

R_i and I_e are the electrical resistance of each layer, and the amplitude of the excitation current respectively.

The side metallic contact is modeled by a fin model which takes into account heat conduction via the SiN layer to the substrate and vice-versa. The substrate is thermally thick and its effect will be contained in what is called «impedance of constriction ». This impedance results from the constriction of thermal flux lines when heat flows through the interface of two mediums of different geometries:

$$Z_{k2}=\frac{8}{3\pi^2\beta_s r\left(1+\frac{8r}{3\pi}\sqrt{\frac{p}{\alpha_s}}\right)} \qquad (2)$$

r is the radius of the contact disc between the two mediums, β_s, and α_s are thermal conductivity and diffusivity of the substrate respectively.

In fact the expression of this impedance depends on the form of temperature and flux distribution on the [0, r] interval, (2) is valid in the case of uniform flux distribution on this interval, the case which is more physical and which we supposed here; There is a difference of just 8% between

the two cases [4]. In addition to the thermal spreading effect inside the substrate, there is also an electrical spreading effect; Joule heating is mainly localized at the interface Buffer-layer/substrate [9]. This electrical spreading is also characterized by a constriction of electrical density flux lines in the substrate. The electrical constriction resistance is calculated, the same way that the thermal resistance is in a steady state, by the equation:

$$R_{sub} = \frac{8}{3\pi^2 \sigma_s r}$$

where r is the radius of the contact disc between the microcooler and the substrate, and σ_s is the electrical conductivity of the substrate.

Another factor, which we demonstrated was an important limiting factor of the performance of the microcooler, is the ohmic contact resistance R_C^{Ohm} between the cap-layer and the metallic layer.

The application of Kirchhoff laws to quadrupoles system (fig.2), allows us to get a matrix relation, which represents the heat transfer in the whole structure in Laplace space, between $\begin{pmatrix}\theta_{C1}\\ \phi_{C1}\end{pmatrix}$ and $\begin{pmatrix}\theta_{C2}\\ \phi_{C2}\end{pmatrix}$, the temperature- flux vectors at the top metallic layer and the interface buffer-layer/ substrate respectively:

$$\begin{pmatrix}\theta_{C1}\\ \phi_{C1}\end{pmatrix} = M_M M_C M_S M_B \begin{pmatrix}\theta_{C2}\\ \phi_{C2} - P_{BS} - J_{sub}\end{pmatrix} - M_M M_C M_S \begin{pmatrix}Z_{1b} J_b\\ J_b\end{pmatrix} - M_M M_C \begin{pmatrix}Z_{1s} J_s\\ J_s\end{pmatrix} - M_M \begin{pmatrix}Z_{1c} J_c\\ J_c + P_{MC} + J_c^{Ohm}\end{pmatrix} - \begin{pmatrix}Z_{1m} J_m\\ J_m\end{pmatrix} \quad (3)$$

The matrix M_i, i=M, C, S, B, represents respectively, the heat transfer matrix of metallic layer, cap layer, superlattice layer and buffer layer.

$P_{MC} = -S_{MC} I_e T_0$, $P_{BS} = -S_{BS} I_e T_0$, $\phi_{C1} = -\frac{\theta_{C1}}{Z_{K1}}$, $\phi_{C2} = \frac{\theta_{C2}}{Z_{K2}}$.

$J_{sub} = \frac{1}{2} R_{sub} I_e^2$, and $J_C^{Ohm} = \frac{1}{2} R_C^{Ohm} I_e^2$. S_{MC}, and S_{BS} are relative Seebeck coefficients at the interfaces metal/cap layer and buffer layer/substrate which include both thermoelectric and thermionic contributions. I_e is the amplitude of the excitation current, and T_0 is the average temperature of the junction that we take equal to room temperature.

Z_{K1} is a thermal impedance which describes thermal leakage from the top side contact of the device. The current probe is supposed to be far away from the device, so that we can neglect heating coming from it. Because the excitation is periodic, it fellows that the temperature of the structure will also be periodic having the same period, especially the junction temperature which we can expand in the form of Fourier series:

$$T = T_0 + \sum_{k=1}^{\infty} T_k \cos\left(k\omega t + \phi_k\right)$$

Each temperature's harmonic is negligible compared to T_0. For this reason only T_0 is taken into account.

V. Harmonic regime

The sample is excited with a wave sine current of frequency f:

$$I(t) = I_e \cos\left(2\pi f t\right)$$

The flow of current gives rise to two effects: the Peltier effect which appears at the same frequency of excitation f, and the Joule effect which appears at frequency of 2f. Both effects being uncorrelated in Fourier space, we can use the principle of superposition, thus we can analyze electrical and thermal responses produced at each frequency separately.

V.1. Thermal response at the first harmonic

If we take into account only the Peltier effect which appears at the two junctions: the metal/SL and the SL/substrate, all Joule sources in (3) vanish. We take the convention that cooling occurs when current flows from the top to the bottom of the structure, and due to the fact that metallic-layer and buffer-layer Seebeck coefficients are less than the cap-layer and silicon substrate Seebeck coefficients respectively, the two interfaces act in the same way, cooling or heating together, we find that cooling occurs if we use the (-) sign in the expressions of P_{MC}, and P_{BS}, which are respectively the amounts of heat absorbed by Peltier effect at the interfaces metal/cap-layer and buffer-layer/silicon substrate.

The resolution of (3) with respect to θ_{C1} gives the temperature variation of the microcooler top side surface. Figure 3 shows comparison between the simulated temperature variation θ_{C1} at f=965Hz (a), and the reflectometric measured variation $\Delta T_{mes\text{-}Ref}$ (b), of the device top side surface, as a function of the excitation current amplitude for different sizes. The simulation reproduces with a good agreement the reflectometric measurements. We should note here that all simulation results are normalized to the temperature variation at zero current that we assume to be zero. Table1 lists all parameters used in our simulation.

Layer	Metallic	Cap	Si/SiGe Superlattice	Buffer	Substrate	SiN
Seebeck Coefficient (μV/K)	8	250	220	220	540	//
Electrical conductivity ($\Omega^{-1}.m^{-1}$)	1×10^7	6.25×10^4	6.25×10^4	5×10^3	5×10^4	0
Thermal conductivity (W/m/K)	63.8	9.6	8	6.1	148	1
Specific heat per unit volume ($J/m^3/K$)	8836 × 516	2673 × 614	2663 × 632	2673 × 614	2329 × 700	3440 × 170

Table 1: Si/SiGe microcooler thermophysical properties used in the simulation.

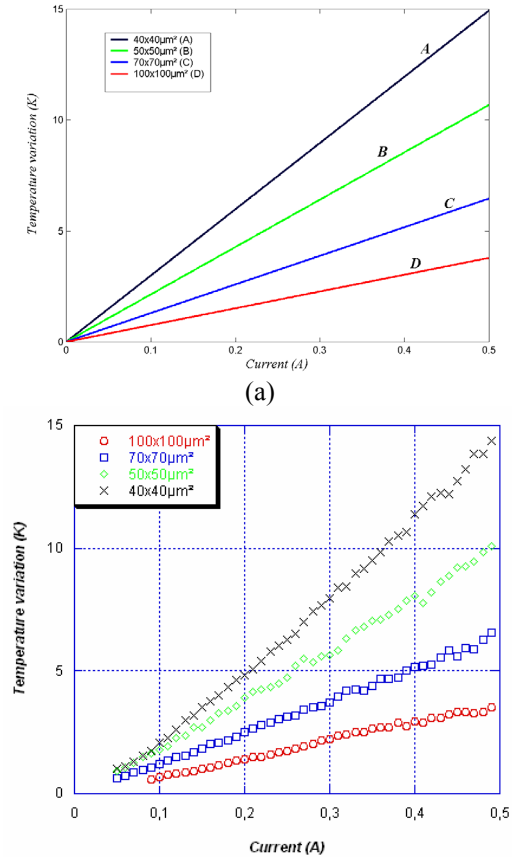

Figure 3: Comparison between simulation results (a), and optical results (b) for Peltier effect (Current response).

Figure 4 (a) shows the simulation of the temperature variation at the top side surface of the microcooler as a function of the excitation frequency for a current amplitude I_e=0.5A. Figure 4 shows a graph (b) of the experimental results obtained using reflectometric technique [9]. The simulation confirms the fact that the time response of the microcooler is <8µs. In fact we found a cut-off frequency $F_{cut-off}$ >20 kHz, which slightly decreases when the device size increases. Previous experimental results [9, 10], have shown that this frequency is mostly independent on the device size.

V.2. Thermal response at the second harmonic

In this case, only the Joule effect will be considered, the later being a delocalized phenomenon, all Peltier sources vanish and the same procedure as above is used.

The resolution of (3) with respect to θ_{C1} allows us to have the temperature variation of the top side surface of the device. Figure 5 (a) and 5 (b) present respectively the simulation curves at 2f=1930Hz and the corresponding reflectometric experimental result as a function of the excitation current amplitude for different sizes. Here also, good agreement between both results is found.

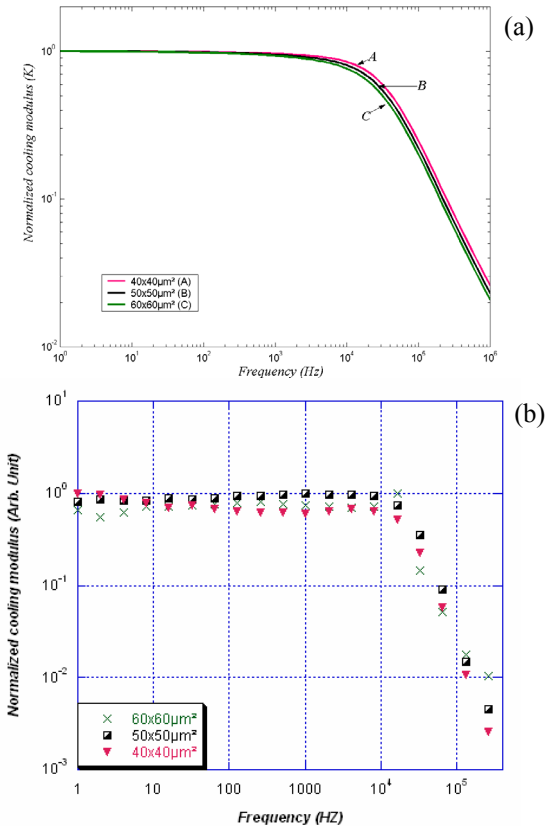

Figure 4: Comparison between simulation results (a), and optical results (b) for Peltier effect (Frequency response).

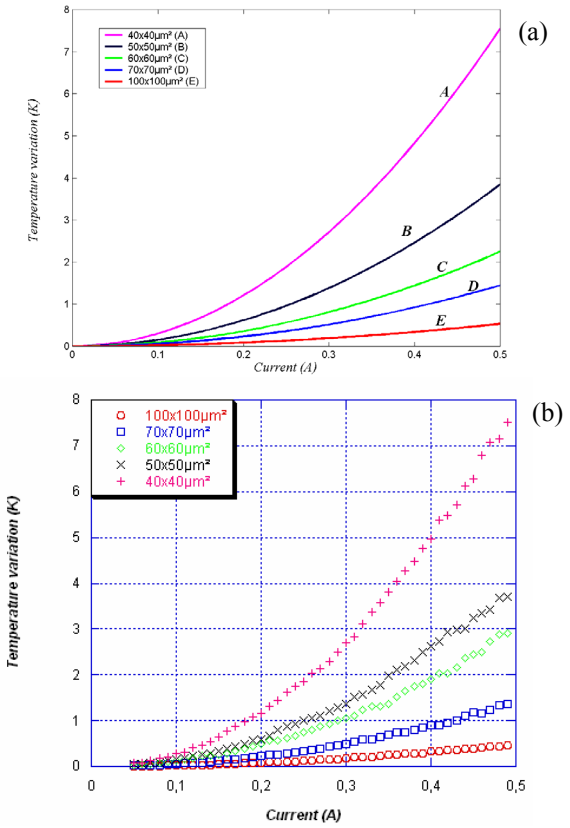

Figure 5: Comparison between simulation results (a), and optical results (b) for Joule effect.

VI. Discussion

In the interval of excitation current amplitude used above, the contribution of the Peltier effect is more important than the Joule effect, in fact the Joule effect is a bulk phenomenon and a delocalized source of heat that appears in all of the structure. By contrast, the Peltier effect appears at the interfaces between two dissimilar materials when current flows through, and in our case the mean part comes from metal/cap layer junction, which is too close from probed top surface. The trend between both effects will rapidly be reversed as current increases. We have also studied the case of steady state. We found that there is an optimum size that produces the better cooling. This result was also found by D. Vashaee et al [3]. Simulation shows that this optimum size is highly dependent of the ohmic contact resistance R_C^{Ohm} between the cap-layer, and the metallic layer. Moreover, the optimum size is only reached when electrical spreading in the substrate is taken into account. Figure 6 shows the simulation of the variation of the maximum cooling as a function of the device area with electrical spreading in the substrate, and without it (the inset), for different values of R_C^{Ohm}. This parameter appears to be the major limiting factor of the device performance.

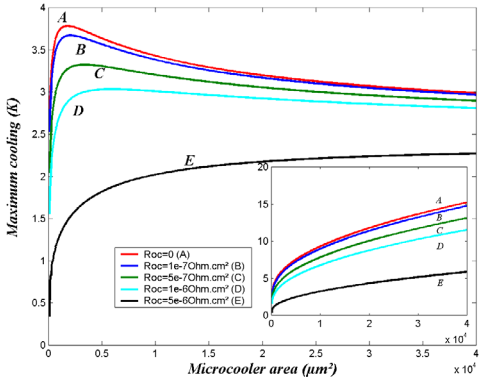

Figure 6: Simulation of the variation of the maximum cooling in DC regime as a function of the device area for several ohmic contact resistances when electrical spreading in the substrate is taking into account. The inset shows what happens if there is no electrical spreading in the substrate.

The existence of this optimum size can be easily explained. The main limiting factor of the cooling efficiency is the total electrical and thermal resistance of the top side of the cooler and of the heat sink at the back side of the substrate. For small devices, both electrical and thermal resistances are larger, the optimal current for maximum cooling is small, and thermal leakage is small too. For large devices, electrical and thermal resistances are small; the optimal current for maximum cooling is big, and thermal leakage is more important. Since heating terms (Joule effect) depends quadratically on current, while cooling terms depends linearly on current, it seems certain that a trade-off of all these parameters gives an optimum device size that has the better cooling.

The small discrepancy between simulation and experiments can be due to the fact that the distance between the current probe and the device was not exactly the same for all microcoolers. This may add an extra source of Joule heating. Also ohmic contact resistance $\mathcal{R}_C^{Ohm}$, package thermal resistance, and all convection-radiation losses sources influence the quality of the simulation. A combination of these factors may explain the discrepancies.

VII. Conclusion

In this paper, we presented detailed description of a thermal quadrupoles model used to simulate a device's top side temperature variation in the AC regime. This model based on the Fourier heat equation demonstrates a great efficiency and compatibility to describe the heat transfer within microcooler devices with a very good accuracy. Both the Peltier and the Joule effects are accessible due to the principle of superposition. The results of simulation were supported by experimental results. The ohmic contact resistance appears to be an important limiting factor of the device performance. We believe that the thermal quadrupoles model could be improved by considering more non-ideal factors. This model in conjunction with optical characterization techniques can help to optimize the performance of Si/SiGe micro-coolers.

VIII. References

[1]: D. M. Row, "Handbook of Thermoelectrics", CRC, 1995.

[2]: D. Vashaee, C. Labounty, X. Fan, G. Zeng, P. Abraham, J. E. Bowers, and A. Shakouri, Proceedings of the SPIE-The International Society for Optical Engineering, vol.4284, 139-144, 2001.

[3]: D. Vashaee, J. Christofferson, Yan Zhang, A. Shakouri, G. Zeng, C. Labounty, X. Fan, J. E. Bowers, and E. Croke, (Unpublished).

[4]: D. Maillet, S. André, J. C. Batsale, A. Degiovanni, and C. Moyne, THERMAL QUADRUPOLES: Solving the Heat Equation through Integral Transforms (John Wiley & Sons, 2000).

[5]: L. D. Patiño-Lopez, PhD thesis, Université Bordeaux 1, (2004).

[6]: Y. Zhang, G. Zeng, R. Singh, J. Christoffersen, E. Croke, J. E. Bowers, and A. Shakouri, 21st International Conference on Thermoelectrics, Long beach, USA, 329-332, August 25-29, 2002.

[7]: J. P. Douglas, Semicond. Sci. Technol. **19,** 75-108, (2004).

[8]: A. Shakouri, E. Y. Lee, D. L. Smith, V. Narayanamurti, and J. E. Bowers, Micro. Therm. Eng, 2, 37, 1998.

[9]: S. Dilhaire, Y. Ezzahri, S. Grauby, W. Claeys, J. Christofferson, Y. Zhang, and A. Shakouri, 23rd International Conference on Thermoelectrics, La Grande Motte, 519-523, August 17-21, (2003).

[10]: A. Fitting, J. Christofferson, A. Shakouri, X. Fan, G. Zeng, C. Labounty, J. E. Bowers, and E. T. Croke, ASME Heat Transfer Division Conference: 2001 IMECE.